

## Supporting Information

# A First Principle Study of a Model Bimolecular Nucleophilic Substitution Reaction Promoted by an Ammonium Catalyst Supported on Oxidized Carbon Black

Maria Voccia<sup>a</sup>, Rosaria Schettini<sup>b</sup>, Maria Rosaria Acocella\*<sup>b</sup>, Sergio Tosoni\*<sup>a</sup>

a) Department of Materials Science, University of Milan-Bicocca, Via Roberto Cozzi 55, 20125, Milan, Italy

b) Department of Chemistry and Biology “A. Zambelli” Chemistry, University of Salerno, Via Giovanni Paolo II, 132, 84084, Fisciano (Sa), Italy

### Computational details.

The exchange-correlation potential was parametrized using the Perdew–Burke–Ernzerhof (PBE) [1] functional within the generalized gradient approximation (GGA). The projector-augmented wave (PAW) [2] approach was utilized to portray the pseudopotentials of the elements. To expand the electronic wave function, a plane-wave basis set with a kinetic cutoff energy of 400 eV was utilized. The cell size is  $22.97808 \text{ \AA} \times 23.35127 \text{ \AA} \times 42.20633 \text{ \AA}$ . A vacuum space of  $\sim 15 \text{ \AA}$  among the slabs was included in the nonperiodic dimension of all calculations involving oCB layer, to hinder the unrealistic interactions among adjacent images. The electronic relaxation convergence threshold between consecutive steps in total energy calculations was less than  $10^{-5} \text{ eV}$ . The truncation criteria for structural optimization (ionic loops and lattice constants) were set to  $0.01 \text{ eV/\AA}$ . The reciprocal space sampling was limited to the Gamma point, given the large size of the adopted supercell. Additionally, long-range dispersion effects were considered based on the D3 approach from Grimme, incorporating the Becke-Johnson damping function.[3-4] The magnetic configuration was left to change during the self-consistent field iterations. Ab Initio Molecular Dynamics (AIMD) simulations were performed using a microcanonical ensemble approach at a constant temperature (100, 200 and 300 K) for a total simulation duration of 1 ps in the case of T= 100 K or 200 K and 1ps in the case of T= 300 K, employing a time step of 1 fs. We explored the impact of solvation method using a self consistent continuum solvation approach within VASPsol++, choosing the water as solvent of reaction as experimentally obtained. We added the entropy effect using the values reported in the literature. [5-11]

**Table S1.** Adsorption energies in solvent phase (water) of the different species reported in Figure 5 and Figure 6.

| $\Delta G$ in Solvent | oCB layer      | $\text{N}(\text{CH}_3)_4\text{Cl}^+$ | NaSCN    | $\text{C}_6\text{H}_5\text{CH}_2\text{Br}$ | $\text{C}_6\text{H}_5\text{CH}_2\text{SCN}$ | NaBr     |
|-----------------------|----------------|--------------------------------------|----------|--|---|----------|
| Energy (eV)           | -1832.10038086 | -92.0576                             | -24.6178 | -91.0354                                   | -109.784                                    | -5.93643 |

**Table S2.** The adsorption energies in solvent phase (water) of the different species reported in Figure 5 and Figure 6.

| $\Delta G$ in Solvent | Adduct in Figure 5a | Adduct in Figure 5b | Adduct in Figure 5c | Adduct in Figure 5d | Adduct in Figure 5e |
|-----------------------|---------------------|---------------------|---------------------|---------------------|---------------------|
| Energy (eV)           | -1924.823185        | -1924.68042162      | -1924.60586598      | -1924.77036634      | -1924.33396299      |

**Table S3.** The adsorption energies in solvent phase (water) of the different species reported in Figure 5 and Figure 6.

| $\Delta G$ in Solvent | Step 1         | Step 2         | Step 3         | Step 4         | Step 5         |
|-----------------------|----------------|----------------|----------------|----------------|----------------|
| Energy (eV)           | -1924.82318545 | -1949.66948855 | -2041.19855419 | -2040.62150891 | -2040.92546948 |

**Table S4.** Comparison of the C-N distances and C-N-C angles of the two quaternary ammonium ions.

|                         | C-N distances (Å)      | C-N-C Angles (°)                           |
|-------------------------|------------------------|--|
| Tetramethylammonium ion | 1.51, 1.51, 1.51, 1.49 | 108.69(2), 108.65(5), 110.23(0), 113.02(2) |
| 2HT ion                 | 1.50, 1.52, 1.50, 1.53 | 108.57(3), 109.60(2), 106.86(8), 113.50(7) |

*Adsorption of tetramethyl ammonium chloride ( $N(CH_3)_4^+Cl^-$ ).*

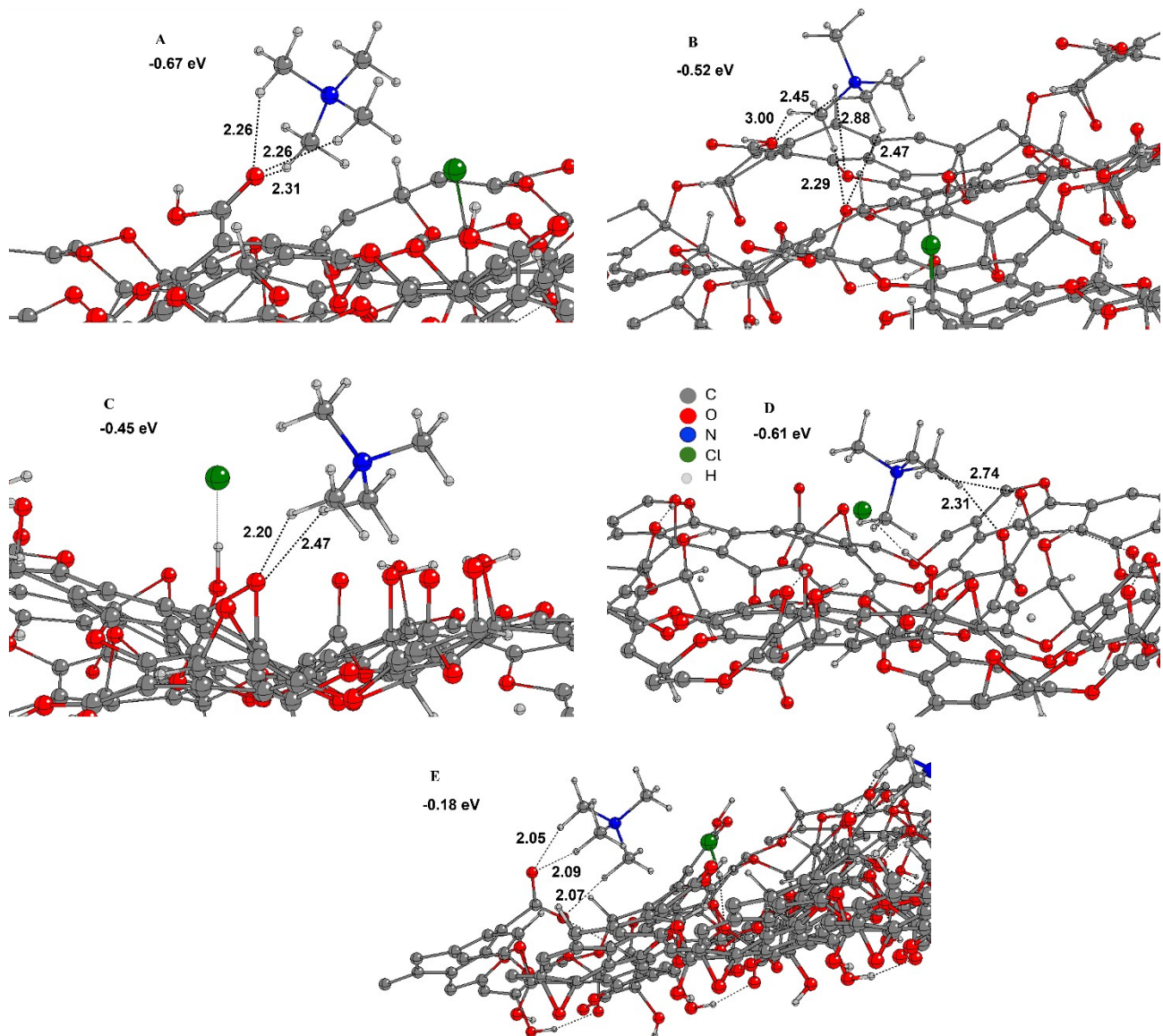


**Figure S1.** Optimized atomic structures for the initial intermediate of  $\text{N}(\text{CH}_3)_4^+$  ion over oCB. The energy costs ( $\Delta\Delta G$ ) in solution (water) of the adduct  $\text{N}(\text{CH}_3)_4^+/\text{oCB}/\text{Cl}^-$  formation are reported in eV. The distances are reported in Å.

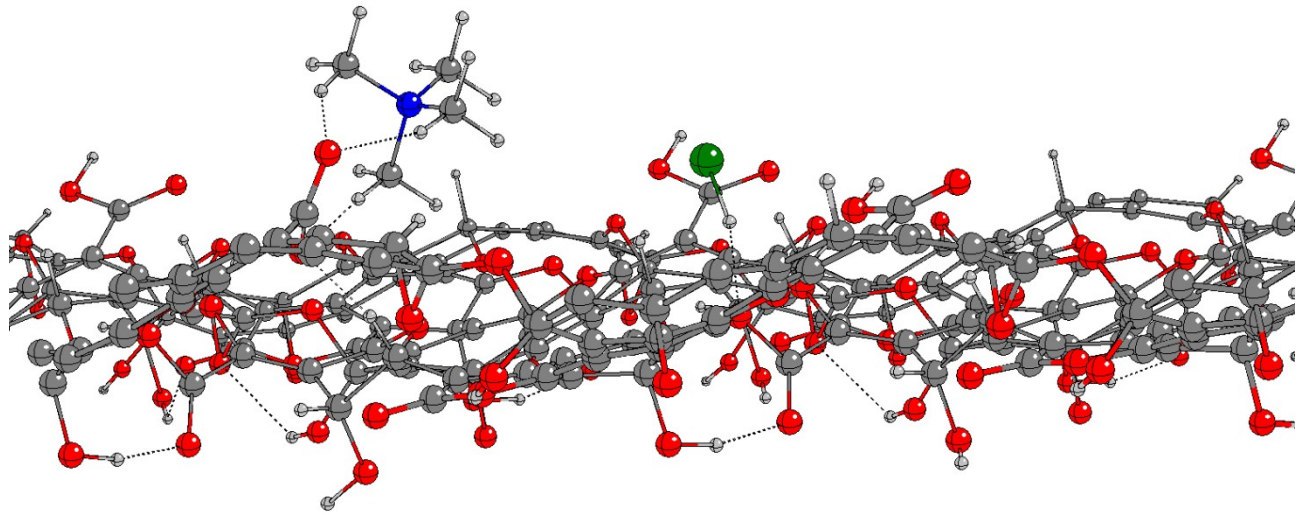


**Figure S2.** Optimized atomic structures for the initial intermediate of  $\text{N}(\text{CH}_3)_4^+$  ion over a carboxylate species.

### The oCB/2HT adducts.

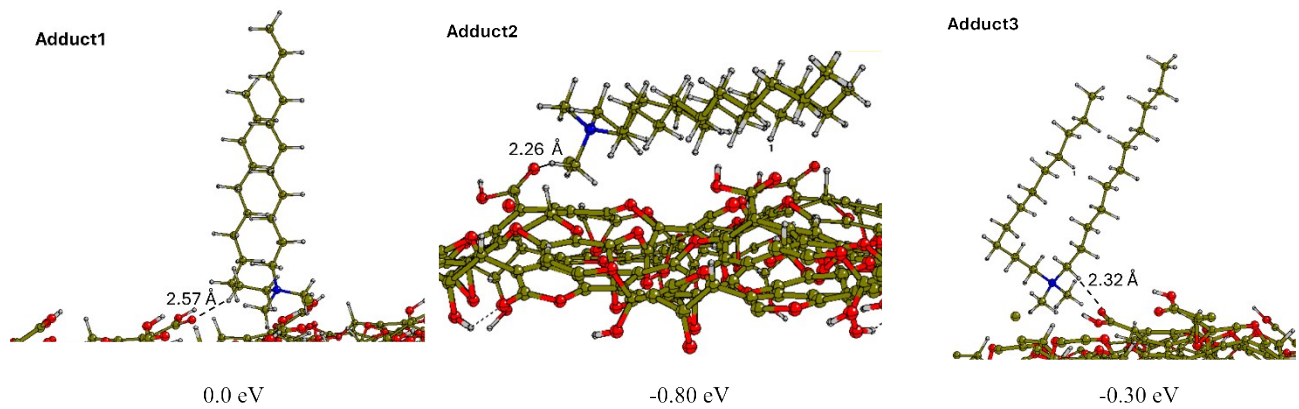


**Figure S3.** Optimized atomic structures for the initial intermediate 2HT over oCB. The energy costs of the adduct 2HT/oCB/ $\text{Cl}^-$  formation in gas phase are reported in eV. The distances are reported in Å.

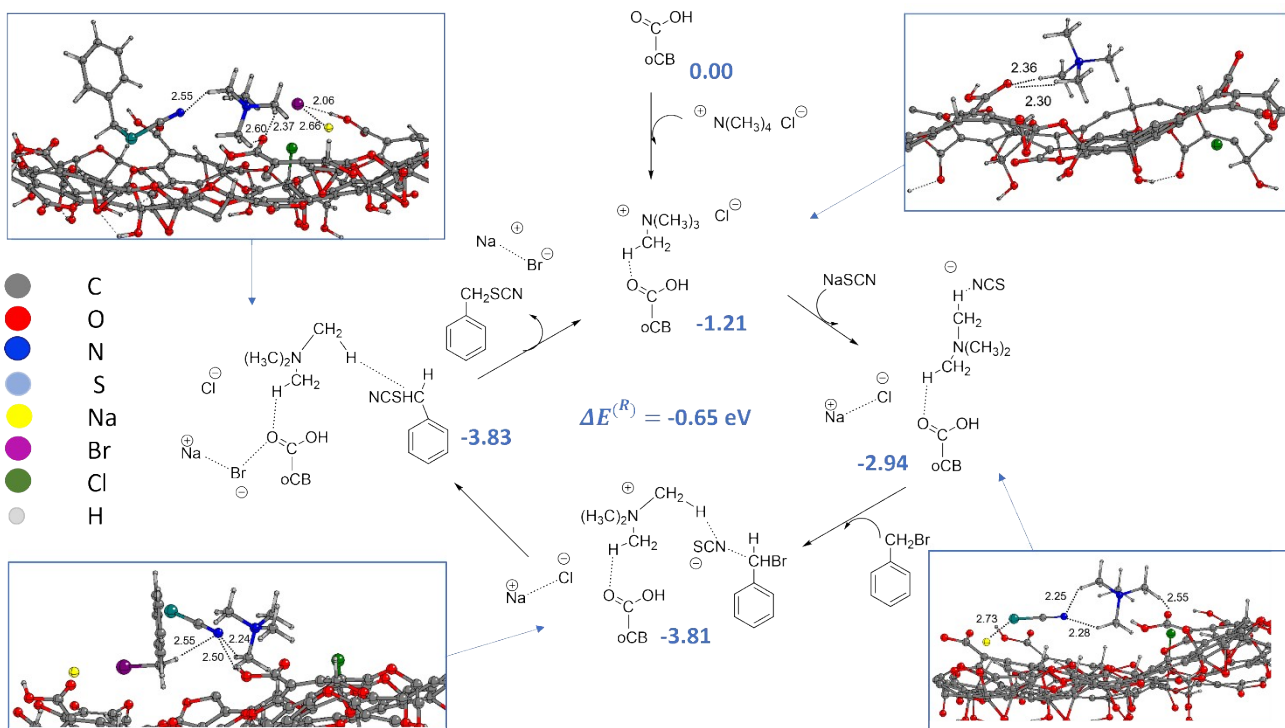


**Figure S4.** DFT-calculated  $S_N2$  substitution nucleophilic reaction in gas phase. The inset shows the structure of each intermediate. Binding energy variations are reported in eV for each step, (gray atoms represent carbon, red atoms represent oxygen, cyan represent sulfur atoms, yellow represents sodium atoms magenta represents bromine atoms, green represent chloride atoms and light gray atom represent hydrogen atoms).

It must be noted that the neglection of the solvent effect in the present model leads to an overestimation of the actual desorption barrier, compare the free energies reported in the main text (Figure 6) with the energies here reported.

## References.

- [1] J. P. Perdew, K. Burke, M. Ernzerhof, *Phys. Rev. Lett.* 1996, **77**, 3865.
- [2] P. E. Blöchl, *Phys. Rev. B* 1994, **50**, 17953.
- [3] S. Grimme, J. Antony, S. Ehrlich, H. Krieg, *J. Chem. Phys.* 2010, **132**, 154104.
- [4] S. Grimme, S. Ehrlich, L. Goerigk, *J. Comput. Chem.* 2011, **32**, 1456–1465.
- [5] W.-Y. Wen, *Journal of Solution Chemistry*, Vol. 2, Nos. 2/3, 1973.
- [6] A. Xenopoulos, J. Cheng, M. Yasuniwa, B. Wunderlich, *Molecular Crystals and Liquid Crystals Science and Technology. Section A. Molecular Crystals and Liquid Crystals*, 1992, **214**:1, 63-79.
- [7] M. L. Miller, M. Doran, *J. Phys. Chem.* 1956, **60**, 2, 186–189.

[8] E. Kaufman, A. Viste, J. Duffy-Matzner, *Journal of Undergraduate Chemistry Research*, 2022, **21**(3), 60.

[9] Benson, S. W.; “Thermochemical Kinetics, Wiley 1976.

[10] N.S. Kurnakov, N.K. Voskresenskaya, *Otdel. Mat. i Estestv. Nauk. Ser. Khim*, 1936, 1936, 439-461.

[11] <https://webbook.nist.gov/cgi/>

---